Journal of Organometallic Chemistry 897 (2019) 23–31

Contents lists available at ScienceDirect

Journal of Organometallic Chemistry

journal homepage: www.elsevier.com/locate/jorganchem

Evaluating ferrocene ions and all-ferrocene salts for electrochemical applications

Briana R. Schrage, Zhiling Zhao, Aliaksei Boika**, Christopher J. Ziegler*

Department of Chemistry, University of Akron, Akron, OH, 44325, USA

ARTICLE INFO

Article history:
Received 2 April 2019
Received in revised form
18 June 2019
Accepted 19 June 2019
Available online 21 June 2019

Keywords:
Ferrocene
Electrochemistry
X-ray structures
Metathesis
Solvent effect

ABSTRACT

The success of applications such as redox flow battery (RFB) technologies is highly dependent on the development of new molecular strategies, and much work has focused on the chemistry of ferrocene compounds as RFB components. This report presents four "all-ferrocene" salts comprised of ferrocene anions and cations and evaluates their solubility and electrochemical properties. The four salts are formed via metathesis reactions employing the (ferrocenemethyl)trimethylammonium cation and mono and bis sulfonate or carboxylate ferrocene anions. We observed that the potentials of the ferrocene components was not only dependent on the substituent, but also on the solvent medium. In particular, the sulfonate and carboxylate ferrocene anions exhibited significant shifts in redox potential between water, propylene carbonate (PC), and DMF. Most notably, in (ferrocenemethyl)trimethylammonium 1,1′-bis(sulfonato)ferrocene, the potentials of the cation and anion reverse, with the anion having a lower potential in aqueous solution and a more positive potential in organic media.

© 2019 Published by Elsevier B.V.

1. Introduction

The increasing importance of renewable sources of energy, in particular with regard to solar energy harvesting, has accelerated the development of new energy storage materials. Recently, the redox flow battery (RFB) approach to energy storage has received increased attention. First developed more than thirty years ago, RFB design has been revisited as a potentially low cost and scalable method for storing potential generated by photovoltaics [1–5]. In particular, the development of new chemical compounds as the redox active components of RFB devices has progressed rapidly. A number of new molecular strategies are being developed and tested, ranging from organic compounds to transition metal species for use in both aqueous and organic media [6–16].

The ferrocene unit (Fig. 1) possesses several potential advantages as a molecular component of RFB devices. This species exhibits very reversible and well understood oxidation and reduction. Additionally, ferrocene can be readily functionalized on one or both rings; such modification can optimize solubility and tune redox potentials. However, in spite of this recent interest in the use of these materials, the structural space of ferrocene derivatives remains largely unexplored for RFB applications [17–23]. In this report, we present several ionic compounds comprised of ferrocene cations and anions, or "all-ferrocene," salts in several solvent systems. A system comprised of multiple ferrocene units could exhibit multiple redox potentials, due to differing substitutions on the ferrocene units. Thus, it is theoretically possible to achieve a stable mixed-valent state, and to obtain a potential from the reaction between the fully oxidized and fully reduced forms of, for example, a bis-ferrocene system.

We have synthesized several all-ferrocene salts, shown in Fig. 1, comprised of the ammonium cation and either a carboxylate or sulfate modified ferrocene. Additionally, we can alter the ferrocene alt ion stoichiometry by using either monofunctionalized or bifunctionalized ferrocenes. The ferrocene salts along with the anionic and cationic precursors were investigated by electrochemical methods. Notably, we observed a dependence on hydrogen bonding in the observed redox potentials for the ferrocene anions in this study. This effect is particularly notable in salts incorporating the bis(sulfonate anion); we previously published a short communication on this chemistry [24]. We observed that, despite the current enthusiasm for ferrocene and ferrocene derivatives, not every ferrocene derivative is equally reversible and stable. Additionally, as we expected, solvent effects play a significant role in the performance of these compounds, and solvent

* Corresponding author.
** Corresponding author.
E-mail addresses: aboika@uakron.edu (A. Boika), ziegler@uakron.edu (C.J. Ziegler).

https://doi.org/10.1016/j.jorganchem.2019.06.023
0022-328X/© 2019 Published by Elsevier B.V.

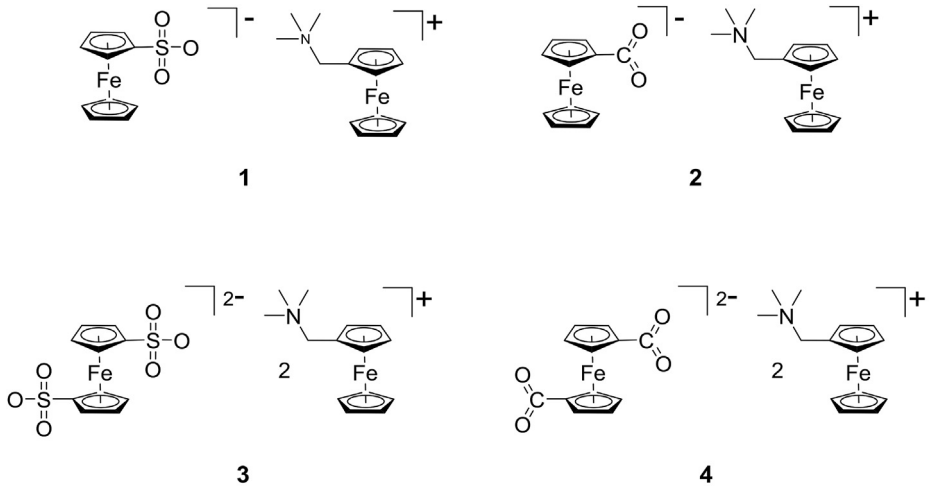

Fig. 1. The structures of all-ferrocene salts **1**–**4**.

choice plays a key role in separating closely spaced redox processes, as well as overall reversibility and stability.

2. Experimental

2.1. General information

All reagents and starting materials were purchased from commercial vendors and used without further purification. Bis ferrocene sulfonic acid was prepared according to the previously published procedure [25]. The mono potassium ferrocenylsulfonate was prepared by an modification of a previously published procedure [26]. Deuterated solvents were purchased from Cambridge Isotope Laboratories and used as received.

NMR spectra were recorded on a Varian 500 MHz spectrometer and chemical shifts were given in ppm relative to residual solvent resonances (^{1}H NMR and ^{13}C NMR spectra). High resolution mass spectrometry experiments were performed on a Bruker MicroTOF-III instrument. Infrared spectra were collected on Thermo Scientific Nicolet iS5 which was equipped with an iD5 ATR.

X-ray intensity data were measured on a Bruker CCD-based diffractometer with dual Cu/Mo ImuS microfocus optics (Cu Kα radiation, λ = 1.54178 Å, Mo Kα radiation, λ = 0.71073 Å). Crystals were mounted on a cryoloop using Paratone oil and placed under a steam of nitrogen at 100 K (Oxford Cryosystems). The detector was placed at a distance of 5.00 cm from the crystal. The data were corrected for absorption with the SADABS program. The structures were refined using the Bruker SHELXTL Software Package (Version 6.1), and were solved using direct methods until the final anisotropic full-matrix, least squares refinement of F2 converged [27]. CCDC numbers 1847169 and 1890052–1890054 contain the supplementary crystallographic data for this paper. These data can be

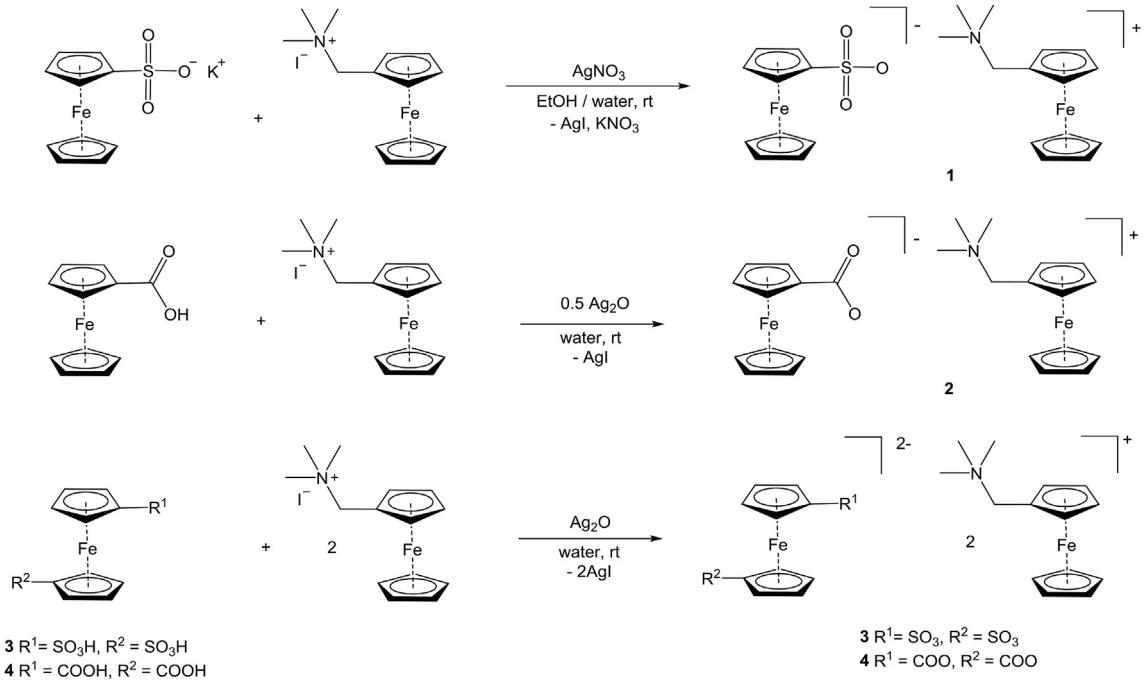

Scheme 1. The syntheses of all ferrocene salts **1**–**4**.

obtained free of charge from The Cambridge Crystallographic Data Centre via www.ccdc.cam.ac.uk/structures.

Electrochemistry measurements were conducted using a CHI 920d potentiostat in a standard three-electrode configuration. A platinum wire was used as an auxiliary electrode. The working electrode used in voltammetry experiments was a platinum disk having a diameter of either 10 μm (microelectrode) or 2 mm (conventional electrode). The nonaqueous Ag/Ag + reference electrode was used by immersing silver wire in degassed dimethylformamide (DMF) or propylene carbonate (PC) solution of 0.01 M $AgNO_3$/0.2 M tetrabutylammonium hexafluorophosphate ($TBAPF_6$). All potentials were referred to the ferrocene methanol/ferrocenium methanol couple. The concentration of analyte was 2 mM, and the supporting electrolyte was 0.2 M $TBAPF_6$ dissolved in DMF or propylene carbonate (PC). All solutions were purged with dinitrogen prior to any electrochemical measurements.

2.2. Syntheses

Synthesis of 1. Ferrocene monosulfonic acid was dissolved in EtOH and neutralized with KOH. The generated mono potassium ferrocenylsulfonate was filtered, and isolated as a yellow solid. The product was washed with cold EtOH, and used without further purification. A sample of 0.25 g (0.82 mmol) of mono potassium

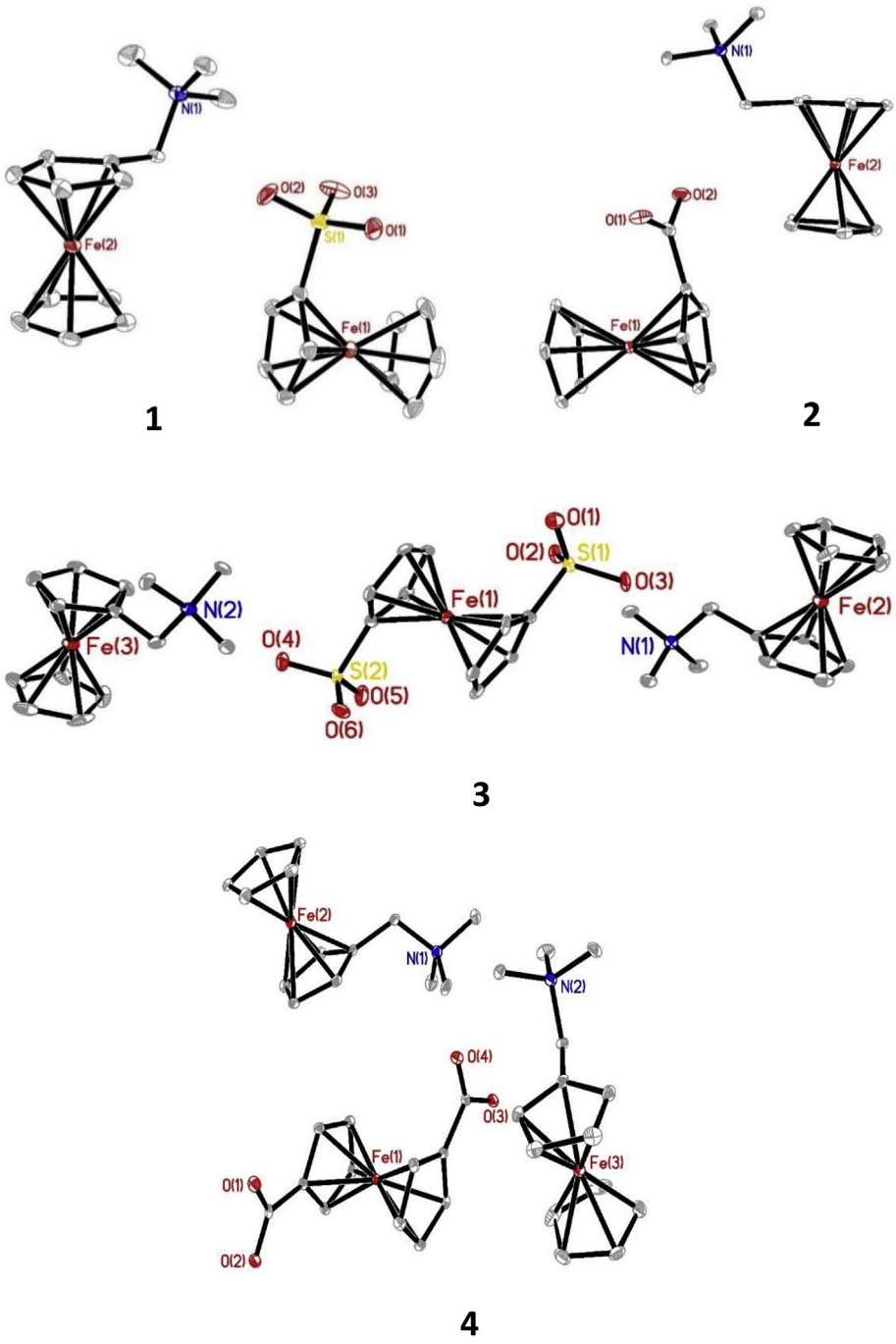

Fig. 2. The structures of compounds **1**–**4** with 35% thermal ellipsoids. Hydrogen atom positions have been omitted for clarity.

ferrocenylsulfonate was dissolved in 2 mL of water and 10 mL of EtOH. To the stirring solution, 0.15 g (0.86 mmol) of $AgNO_3$ was added and the solution turned green. After the solids were dissolved, 0.33 g (0.86 mmol) of (ferrocenemethyl)trimethylammonium iodide were added to the mixture. After 1 h of stirring at room temperature, the AgI precipitate was filtered. The filtrate was collected and the solvent was removed by rotary evaporation. The residue was precipitated with the addition of ether, and the resultant solid was filtered and washed with cold DCM. Crystals suitable for X-ray diffraction were grown by vapor diffusion of MeOH into a hexane solution.

(1). Yield: 0.37 g (86%). IR (S–O stretch, cm^{-1}): 891 (w), (SO stretch, cm^{-1}): 1355 (br, m), 1177(s). Hi-res ESI MS (positive mode) calcd $C_{24}H_{29}Fe_2NO_3S$ 523.0568 m/z, found 523.0553. ^1H NMR (500 MHz, d_6 - DMSO): δ = 4.49 (t, 2H, H on $C_5\mathbf{H}_4$), 4.37 (m, 4H, H on $C_5\mathbf{H}_4$, and $C\mathbf{H}_2$), 4.29 (s, 2H, H on $C_5\mathbf{H}_4$), 4.24 (m, 5H on Cp), 4.18 (s, 5H on Cp), 4.05 (s, 2H, H on $C_5\mathbf{H}_4$), 2.90 (s, 9H, $C\mathbf{H}_3$). $^{13}C\{^1H\}$ NMR (125 MHz, d_6 - DMSO): δ = 97.1, 73.4, 72.1, 70.1, 69.5, 69.1, 67.2, 67.1, 65.6, 51.5 ($\mathbf{C}H_3$).

Synthesis of 2–4. The procedure for the synthesis of **3**–**4** is the same as **2** except 0.72 mmol of 1,1′- bis ferrocene sulfonic acid, and 0.91 mmol of 1,1′-bis ferrocene carboxylic acid were used. To generate compound **2**, 0.25 g (1.09 mmol) of ferrocene carboxylic acid was dissolved in 10 mL of water. To this stirring solution, 0.126 g (0.54 mmol) of Ag_2O, and 0.42 g (1.09 mmol) of (ferrocenemethyl)trimethylammonium iodide were added. The reaction flask was wrapped in foil in the dark and left to stir at room temperature for 24 h. The AgI was filtered, and the filtrate was freeze dried. The residue was dissolved in MeOH and precipitated with the addition of ether. The generated solid was filtered and washed with cold DCM. Crystals suitable for X-ray diffraction were grown by vapor diffusion of hexane into a MeOH solution, THF into a MeOH solution, and water evaporation for **2**–**4** respectively.

(2). Yield: 0.40 g (75%). IR (CO stretch, cm^{-1}): 1377(vs), 1571 (vs). Hi-res ESI MS (positive mode) calcd $C_{25}H_{19}Fe_2NO_2$ 487.0898 m/z, found 487.0897. ^1H NMR (500 MHz, d_6 - DMSO): δ = 4.49 (t, 2H, H on $C_5\mathbf{H}_4$), 4.38 (m, 4H, H on $C_5\mathbf{H}_4$, and $C\mathbf{H}_2$), 4.34 (t, 2H, H on $C_5\mathbf{H}_4$), 4.24 (s, 5H on Cp), 4.01 (s, 5H on Cp), 3.99 (s, 2H, H on $C_5\mathbf{H}_4$), 2.91 (s, 9H, $C\mathbf{H}_3$). $^{13}C\{^1H\}$ NMR (125 MHz, d_6 - DMSO): δ = 170.6 (C═O), 84.5, 73.3, 71.9, 69.9, 69.6, 68.9, 68.3, 67.6, 65.4, 51.3 ($\mathbf{C}H_3$).

(3). Yield: 0.55 g (89%). IR (SO stretch, cm-1): 1383 (m), 1175 (s). Hi-res ESI MS (positive mode) calcd $C_{38}H_{48}Fe_3N_2O_6S_2$ 861.1083 m/z, found 861.0950. ^1H NMR (300 MHz, d_6 -DMSO): δ = 4.50 (s, 4H, H on $C_5\mathbf{H}_4$), 4.39 (s, 4H, H on $C_5\mathbf{H}_4$), 4.38 (s, 4H, $C\mathbf{H}_2$), 4.31 (s, 4H, H on $C_5\mathbf{H}_4$), 4.24 (s, 10H, Cp), 4.11 (s, 4H, H on $C_5\mathbf{H}_4$), 2.92 (s, 18H, $C\mathbf{H}_3$). $^{13}C\{^1H\}$ NMR (125 MHz, d_6 − DMSO): δ = 50.92, 65.00, 67.50, 68.50, 69.52, 69.91, 71.49, 72.78.

(4). Yield: 0.52 g (73%). IR (CO stretch, cm^{-1}): 1381 (vs), 1555 (vs). ESI MS (positive mode) calcd $C_{14}H_{21}FeN$ 259.1018 m/z, found 259.1045 $[M+H]^+$, calcd $C_{12}H_{10}FeNaO_4$ 296.9821 m/z, found 296.9873 $[M+Na]^+$. ^1H NMR (500 MHz, d_6 - DMSO): δ = 4.51 (s, 4H, H on $C_5\mathbf{H}_4$), 4.43 (m, 4H, H on $C_5\mathbf{H}_4$, and $C\mathbf{H}_2$), 4.37 (s, 4H, H on $C_5\mathbf{H}_4$), 4.30 (m, 4H, H on $C_5\mathbf{H}_4$), 4.24 (s, 10H on Cp), 3.84 (s, 4H, H on $C_5\mathbf{H}_4$), 2.96 (s, 18H, $C\mathbf{H}_3$). $^{13}C\{^1H\}$ NMR (125 MHz, d_6 - DMSO): δ = 171.7 (C═O), 83.6, 73.3, 71.9, 70.1, 69.9, 68.9, 68.4, 65.4, 51.4 ($\mathbf{C}H_3$).

3. Results and discussion

The syntheses of the all-ferrocene salts (compounds **1**–**4**) are carried out via straightforward ion metatheses reactions. The ammonium and carboxylic acid modified ferrocenes can be readily synthesized [28–32] or purchased from chemical vendors. The mono and bis sulfonate modified ferrocenes can be produced via the reaction of chlorosulfonic acid with ferrocene, with the desired products formed by manipulation of reaction conditions [25,26,33]. We have used these compounds over the past few years as precursors to synthesize a variety of sulfonamide and sulfonyl compounds [25,34,35]. Scheme 1 shows the synthetic methods used to generate compounds **1**–**4**. The all-ferrocene salts are produced via use of silver ferrocene salts as *in situ* intermediates, which upon reaction with the ferrocene trimethylammonium iodides, afford the desired all-ferrocene salts as pure crystalline materials. The monosulfonate salt uses silver nitrate as the source of the metathesis reagent, while the remaining three preparations employ silver oxide in either one half or one equivalent depending on the charge of the anion. These compounds were fully characterized to confirm their composition, including by single crystal X-ray diffraction for all of the compounds, the structures of which are shown in Fig. 2. The salts exhibit the expected structural features for these ions, in good agreement with previously published structure elucidations [36–43].

One of the key properties of any redox active component of RFB is solubility; without sufficient solubility, optimal energy density cannot be achieved. Table 1 lists the solubility of compounds **1**–**4** in several organic solvents and in water; solubilities were determined after sonication for 10 min at 293 K and 1 atm of pressure. All four salts are reasonably soluble in both aqueous and organic media. The best solubilities are observed in aqueous solution, and in organic solvents larger solubilities are seen in the polar solvents like PC, DMF and DMSO. Once concern is the lower solubility in MeCN, which is in contrast with many ferrocene derivatives. However, with regard to aqueous solubility, the salts exhibit significantly increased solubility versus compounds such as ferrocene methanol. Additionally, hydrogen bonding interactions may also be playing a role in solvation, as we have observed a notable effect of these intermolecular forces on the oxidation potential of the anions.

We investigated the electrochemistry of solutions of the single ferrocene cations and anions, as well as salts **1**–**4**. The electrochemical behaviors of the ammonium and carboxylate modified ferrocenes have been explored; in particular the ammonium cation has been used in a wide variety of electrochemical applications [18,44,45]. In contrast, the electrochemistries of the mono and bis-sulfonate modified ferrocene have not been as extensively investigated [46,47]. Table 2 shows the half wave potentials versus ferrocenium methanol/ferrocene methanol redox couple for the five

Table 1
Solubilities of compounds **1**–**4** (units: mM) at 293 K and 1 atm.

	H_2O	PC	DMSO	DMF	MECN
1	12	8.7	7.1	8.3	0.6
2	16	10	10	10	2.5
3	21	4.8	4.5	3.0	0.6
4	25	12	11	12	1.7

Table 2
Half-wave potentials in mV versus ferrocenium methanol/ferrocene methanol couple using a 2 mm dia. Pt electrode. The values were determined by averaging the peak potentials, unless a clear irreversibility is observed, in which case we estimated the half-wave potential values. Cyclic voltammograms are shown in the supplemental information in Figures S14, S16 and S18.

H_2O	**1**	**2**	**3**	**4**
cation	124			
anion	120	37	346	170
PC				
cation	120			
anion	−60	126	−21	~300
DMF				
cation	78			
anion	−110	76	−120	~290

ions. Figs. S14–S19 show the cyclic voltammograms of the ammonium cation, mono carboxylate, bis carboxylate, mono sulfonate, and bis-sulfonate modified ferrocene ions respectively in water, DMF, and PC solutions. We note several trends in the degree of reversibility and the potentials in these solvent systems. First, the carboxylate salts clearly exhibit solvent-dependent stability issues in organic media, as seen in the lack of reversibility. Second, all of the ferrocenes undergo significant shifts in redox potential depending on the solvent. In H_2O and PC, the half wave potentials of the ferrocene ammonium cation are 124 and 120 mV versus ferrocenium methanol/ferrocene methanol, while in DMF the potential shifts to the lower value of 78 mV. For the anions, in most cases the potential shifts to more negative values going from water to PC or DMF. This effect is most clearly seen in the bis-sulfonate

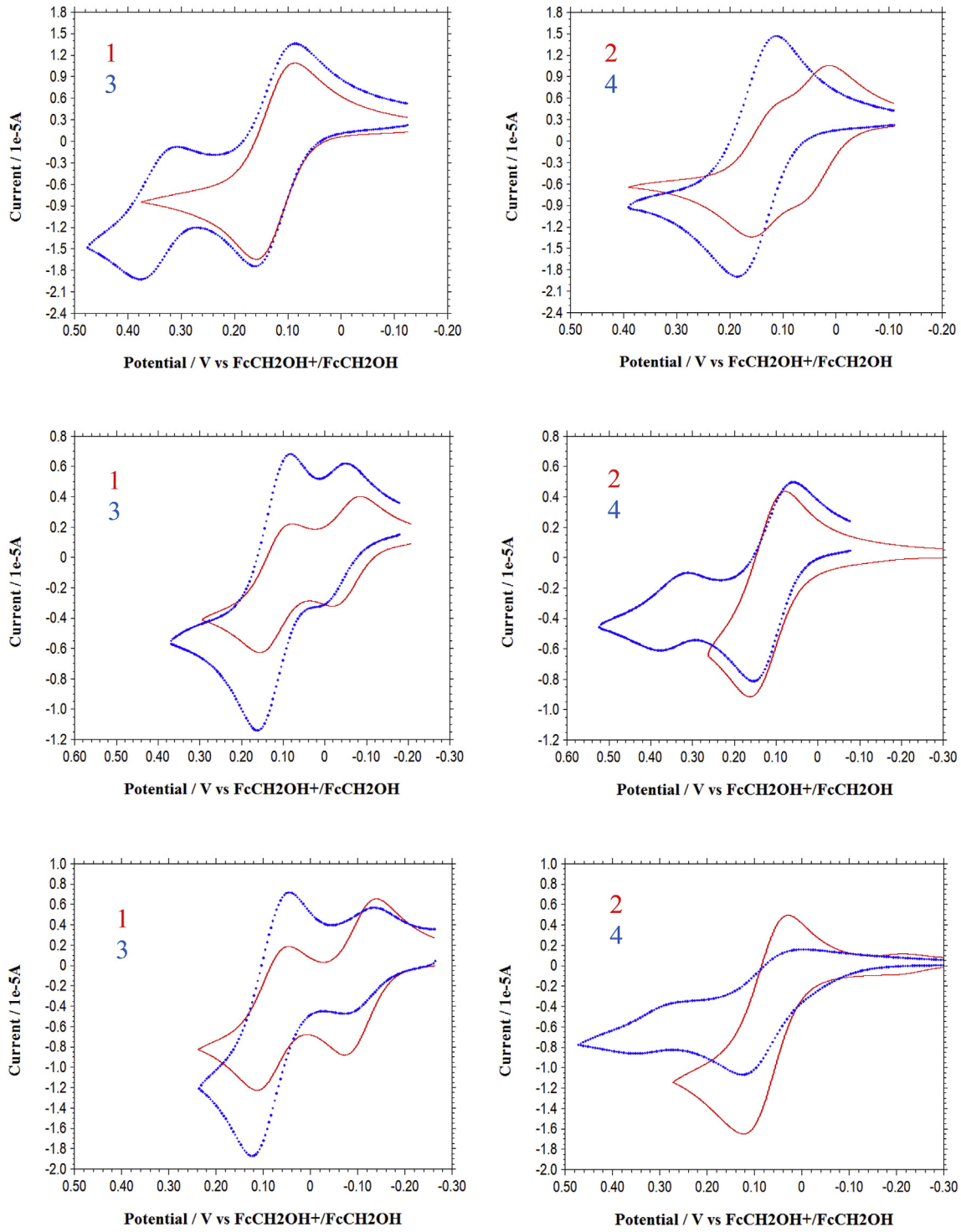

Fig. 3. Cyclic voltammograms of all-ferrocene salts **1**–**4** (2 mM) measured on 2 mm dia. Pt at scan rate 60 mV/s. Top: aqueous solution with 0.2 M KCl; Middle: PC solution with 0.2 M $TBAPF_6$; Bottom: DMF solution with 0.2 M $TBAPF_6$. Salts **1** and **2**: red solid curves; salts **3** and **4**: blue dotted curves. Ferrocene methanol has relative potential of −29 mV and −24 mV to ferrocene in PC and DMF respectively. (For interpretation of the references to colour in this figure legend, the reader is referred to the Web version of this article.)

modified ferrocene; we initially reported this solvent dependent redox behavior in a communication [24]. One exception to this trend is the monocarboxylate anion, which increases in potential in organic solvents.

In the salt systems, we observe some changes in the behavior from that of the individual ions themselves. The cyclic voltammograms for **1**–**4** are shown in Figs. 3 and 4 (2 mm Pt electrode and 10 μm Pt microelectrode respectively). In compounds **1** and **4** in water and in compound **2** in DMF and PC, we observe simultaneous oxidations in both cation and anion, and thus cannot differentiate the half potentials of each ionic component. For compound **1** in water and compound **2** in PC and DMF, this lack of separation is clearly expected, as the potentials of the ferrocenes are effectively identical when alone with an inert counterion in solution. However,

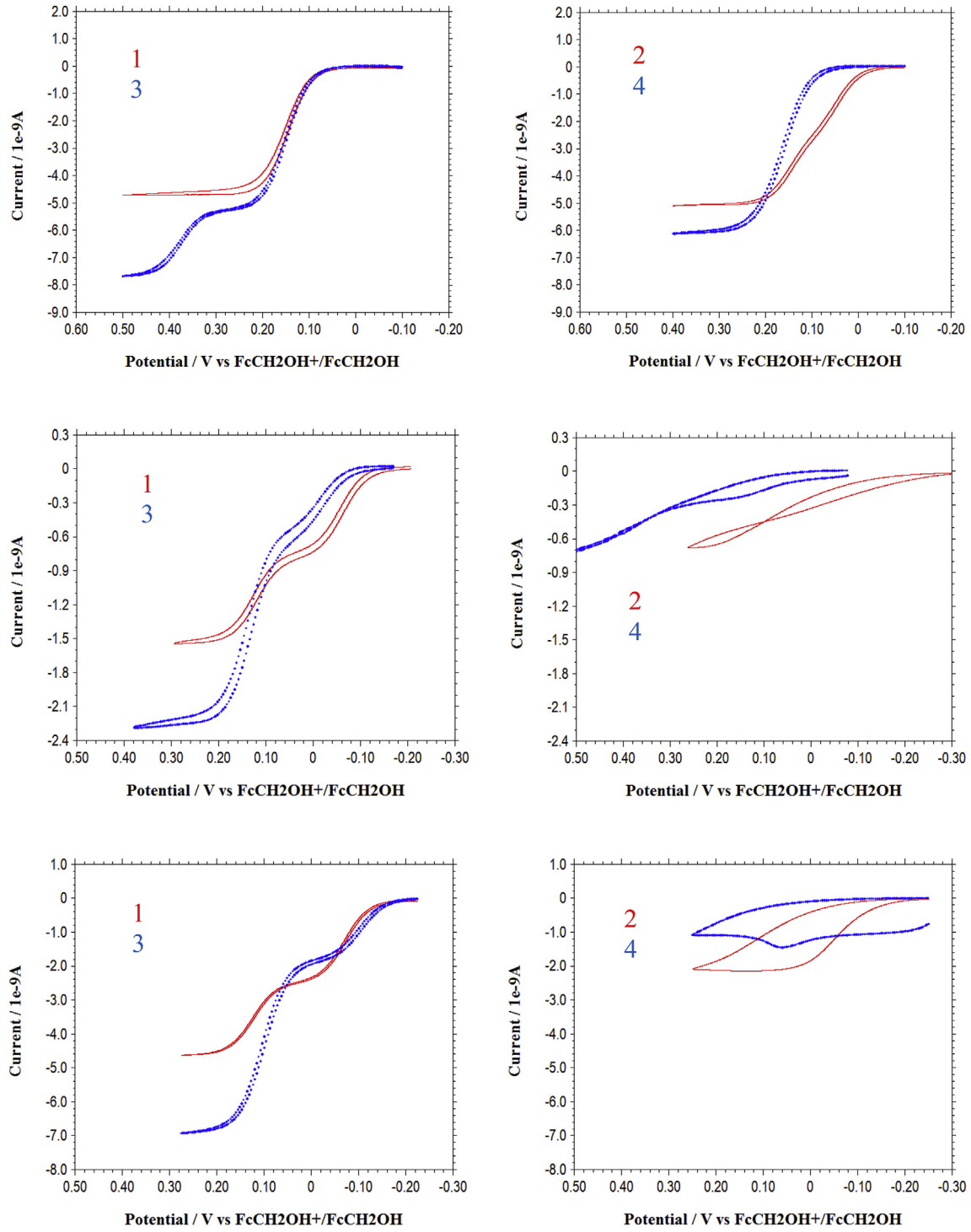

Fig. 4. Cyclic voltammograms of all-ferrocene salts **1**–**4** (2 mM) measured on 10 μm dia. Pt at scan rate 20 mV/s. Top: aqueous solution with 0.2 M KCl; Middle: PC solution with 0.2 M $TBAPF_6$; Bottom: DMF solution with 0.2 M $TBAPF_6$. Salts **1** and **2**: red solid curves; salts **3** and **4**: blue dotted curves. Ferrocene methanol has relative potential of −29 mV and −24 mV to ferrocene in PC and DMF respectively. (For interpretation of the references to colour in this figure legend, the reader is referred to the Web version of this article.)

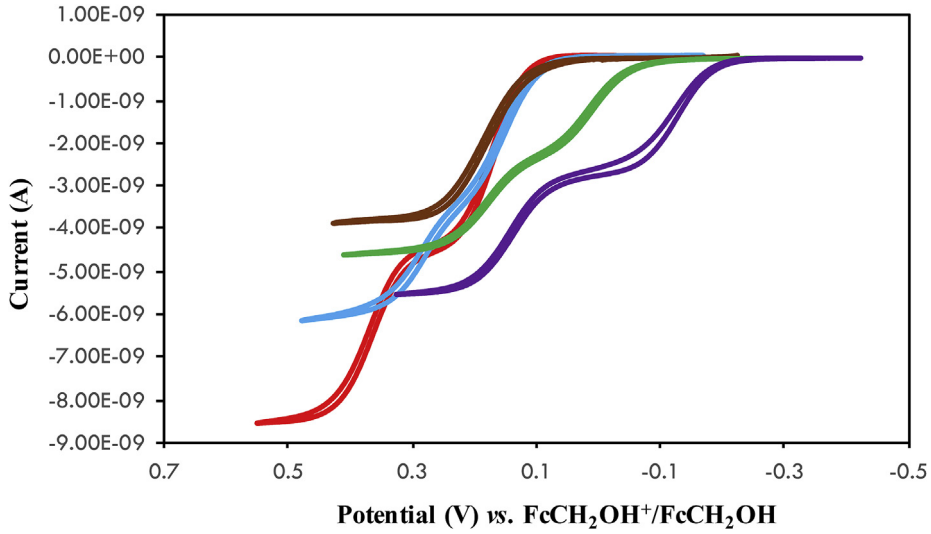

Fig. 5. Cyclic voltammograms of bis sulfonate ammonium salt (2 mM) in DMF-water mixtures with molar fraction of water 1 (red curve), 0.97 (blue), 0.74 (brown), 0.32 (green) and 0 (purple). No supporting electrolyte was added to the mixtures. Working electrode – 10 μm Pt disk, scan rate 20 mV/s. (For interpretation of the references to colour in this figure legend, the reader is referred to the Web version of this article.)

for salt **4** there is a ~45 mV separation between the two ferrocene ions when separate with an inert counterion, and yet two separate redox processes are not observed upon combination. This is explained by the inability of the cyclic voltammetry experiment to separate the two redox processes since the difference of the standard potentials is < 100 mV [48].

The most striking changes observed in these salt systems are seen in the oxidation potentials of the anionic components. For the sulfonate salts **1** and **3**, the oxidation potentials of the anions shift to negative potentials in the organic solvents PC and DMF. The largest shift is observed for the bis-sulfonate ferrocene anion, which moves approximately 450 mV from H_2O to DMF. Initially we ascribed this shift due to the changes in intermolecular interactions with the solvent medium, such as dielectric constant changes or hydrogen bonding interactions. Measuring the redox potential in PC allowed us to help elucidate the nature of these interactions, as PC has a similar dielectric constant as H_2O but lacks the ability to be a hydrogen bond donor. Notably, the redox potentials of the sulfonate anions do move but are closer to those of DMF than to those of water. Thus, we hypothesize that hydrogen bonding plays a more significant role in modulating the potential of the sulfonate anions than does the polarity of the solvent. As for the carboxylate anions, the effects of solvent interactions are more difficult to elucidate, due to their lack of reversibility. The lack of reversibility of ferrocene carboxylate anions is well known [49,50]. However, we do observe that in the carboxylate salts **2** and **4**, the redox potential is most positive in PC, intermediate in DMF, and lowest in H_2O.

Previously, we presented the redox properties of compound **3**, and we observed that it is possible to tune its redox response to exhibit only one oxidation peak. Fig. 5 shows the cyclic voltammagrams of compound **3** at various molar fractions of water and DMF. At a molar fraction of water x = 0.74, we observe only one oxidation wave instead of the two as seen in only water or DMF. There is clearly a change in the values of the limiting currents in

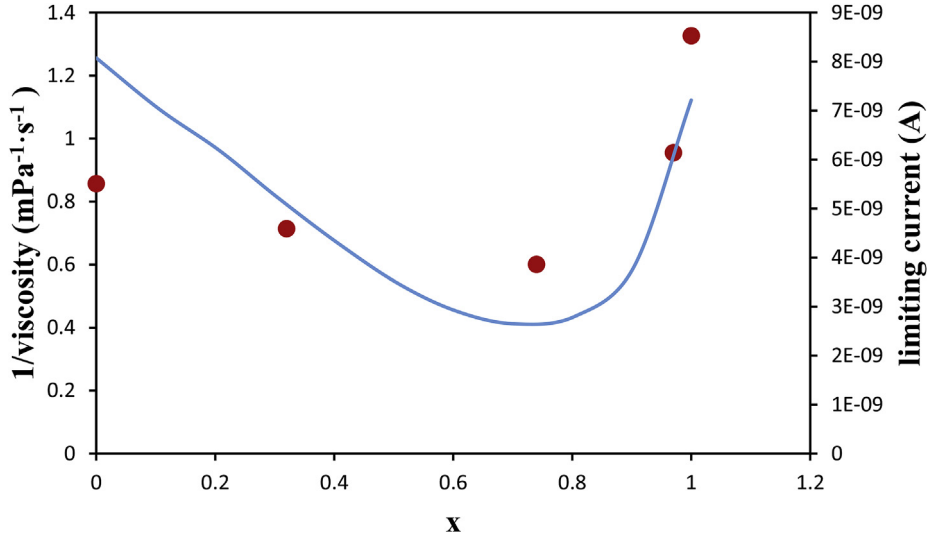

Fig. 6. Limiting current (data points) and inverse solution viscosity (curve) as a function of the molar fraction of water (X) in the DMF-water mixtures. The values of the limiting current were determined from the results in Fig. 5. The viscosity data were taken from Ref. [48].

these experiments dependent on the solution composition. The main effect is easily attributable to changes in solution viscosity, which is dependent on the solvent composition. Fig. 6 shows a plot of the inverse solution viscosity and the limiting current values versus the solvent composition; the viscosity data for the water-DMF mixtures were taken from the literature [51]. The inverse viscosity was used since the diffusion coefficients are inversely proportional to the solution viscosity according to the Stokes-Einstein equation. On the graph, the limiting current points line up quite well with the inverse viscosity curve, in support of our hypothesis. Some disagreement between the two sets of values is expected due to the presence of the migration effect, since no supporting electrolyte was added to these mixtures.

In conclusion, we present a study into the syntheses and electrochemical activity of a series of all-ferrocene salts. The four salts, comprised of (ferrocenemethyl)trimethylammonium cations and either carboxylate or sulfonate ferrocene anions, can be readily synthesized via simple metathesis reactions. Depending on the identity of the anions and cations in compounds **1**–**4**, we observe different degrees of separation between the oxidation potentials of the ferrocene components. The potentials of the ions in salts **1**–**4** are highly dependent on solvent conditions, and comparisons between water, PC, and DMF reveal that hydrogen bonding in addition to other solvent interactions may be playing a key role in modulating the redox potentials on the anionic components of these salts. Clearly, the choices of solvent and ferrocene ions will have a significant role in any redox flow battery design. With regard to RFB materials, the system with the largest difference in potential between ferrocene cation and anion is compound **3**, and this salt, depending on the solvent choice, could form a stable mixed valent state. It is notable that the ferrocene sulfonates have improved solubility versus ferrocene methanol and are reversible, and this is the first evaluation of these compounds for possible energy storage applications. We are continuing our investigations into these compounds and the effects of solvent and solvation on potential.

Acknowledgement

The authors would like to acknowledge The University of Akron and the National Science Foundation (CHE-1665267) for support of this research.

Appendix A. Supplementary data

Supplementary data to this article can be found online at https://doi.org/10.1016/j.jorganchem.2019.06.023.

References

[1] G.L. Soloveichik, Flow batteries: current status and trends, Chem. Rev. 115 (2015) 11533–11558, https://doi.org/10.1021/cr500720t.
[2] Z. Qi, G.M. Koenig, Review Article: flow battery systems with solid electroactive materials, J. Vac. Sci. Technol. B, Nanotechnol. and Microelectron. Mater. Process. Meas. Phenom. 35 (2017) 040801, https://doi.org/10.1116/1.4983210.
[3] M.H. Chakrabarti, S.A. Hajimolana, F.S. Mjalli, M. Saleem, I. Mustafa, Redox flow battery for energy storage, Arabian J. Sci. Eng. 38 (2013) 723–739, https://doi.org/10.1007/s13369-012-0356-5.
[4] A.Z. Weber, M.M. Mench, J.P. Meyers, P.N. Ross, J.T. Gostick, Q. Liu, Redox flow batteries: a review, J. Appl. Electrochem. 41 (2011) 1137–1164, https://doi.org/10.1007/s10800-011-0348-2.
[5] P. Alotto, M. Guarnieri, F. Moro, Redox flow batteries for the storage of renewable energy: a review, Renew. Sustain. Energy Rev. 29 (2014) 325–335, https://doi.org/10.1016/j.rser.2013.08.001.
[6] J. Rajpurohit, A. Upadhyay, C. Das, R. Dubey, S. Vaidya, V. Krishnan, A. Kumar, M. Shanmugam, Unusual methylenediolate bridged hexanuclear ruthenium(III) complexes: syntheses and their application, Inorg. Chem. 57 (2018) 14967–14982, https://doi.org/10.1021/acs.inorgchem.8b02780.
[7] A. Petty II, S. Mann, A. Dumitrascu, K. Olson, T.F. Guarr, Multifunctional pyridinium systems for nonaqueous redox flow batteries, ECS Trans. 80 (2017) 1241–1255, https://doi.org/10.1149/08010.1241ecst.
[8] C. DeBruler, B. Hu, J. Moss, X. Liu, J. Luo, Y. Sun, T.L. Liu, Designer two-electron storage viologen anolyte materials for neutral aqueous organic redox flow batteries, Chem 3 (2017) 961–978, https://doi.org/10.1016/j.chempr.2017.11.001.
[9] G.M. Duarte, J.D. Braun, P.K. Giesbrecht, D.E. Herbert, Redox non-innocent bis(2,6-diimine-pyridine) ligand-iron complexes as anolytes for flow battery applications, Dalt. Trans. 46 (2017) 16439–16445, https://doi.org/10.1039/C7DT03915H.
[10] L. Xia, L. Yu, D. Hu, G.Z. Chen, Electrolytes for electrochemical energy storage, Mater. Chem. Front. 1 (2017) 584–618, https://doi.org/10.1039/C6QM00169F.
[11] A. Shimizu, K. Takenaka, N. Handa, T. Nokami, T. Itoh, J. Yoshida, Liquid quinones for solvent-free redox flow batteries, Adv. Mater. (Weinheim, Ger). 29 (2017), https://doi.org/10.1002/adma.201606592 n/a.
[12] P. Navalpotro, J. Palma, M. Anderson, R. Marcilla, A membrane-free redox flow battery with two immiscible redox electrolytes, Angew. Chem. Int. Ed. 56 (2017) 12460–12465, https://doi.org/10.1002/anie.201704318.
[13] Y. Li, J. Sniekers, J. Malaquias, X. Li, S. Schaltin, L. Stappers, K. Binnemans, J. Fransaer, I.F.J. Vankelecom, A non-aqueous all-copper redox flow battery with highly soluble active species, Electrochim. Acta 236 (2017) 116–121, https://doi.org/10.1016/j.electacta.2017.03.039.
[14] C.G. Armstrong, K.E. Toghill, Cobalt(II) complexes with azole-pyridine type ligands for non-aqueous redox-flow batteries: tunable electrochemistry via structural modification, J. Power Sources 349 (2017) 121–129, https://doi.org/10.1016/j.jpowsour.2017.03.034.
[15] Y. Zhao, Y. Ding, Y. Li, L. Peng, H.R. Byon, J.B. Goodenough, G. Yu, A chemistry and material perspective on lithium redox flow batteries towards high-density electrical energy storage, Chem. Soc. Rev. 44 (2015) 7968–7996, https://doi.org/10.1039/C5CS00289C.
[16] T. Janoschka, M.D. Hager, U.S. Schubert, T. Janoschka, M.D. Hager, U.S. Schubert, N. Martin, An aqueous redox-flow battery with high capacity and power: the TEMPTMA/MV system, Angew Chem. Int. Ed. Engl. 55 (2016) 14427–14430.
[17] B. Hwang, M.-S. Park, K. Kim, Ferrocene and cobaltocene derivatives for non-aqueous redox flow batteries, ChemSusChem 8 (2015) 310–314, https://doi.org/10.1002/cssc.201403021.
[18] L. Cosimbescu, X. Wei, M. Vijayakumar, W. Xu, M.L. Helm, S.D. Burton, C.M. Sorensen, J. Liu, V. Sprenkle, W. Wang, Anion-tunable properties and electrochemical performance of functionalized ferrocene compounds, Sci. Rep. 5 (2015) 14117, https://doi.org/10.1038/srep14117.
[19] J. Friedl, M.A. Lebedeva, K. Porfyrakis, U. Stimming, T.W. Chamberlain, All-fullerene-based cells for nonaqueous redox flow batteries, J. Am. Chem. Soc. 140 (2018) 401–405, https://doi.org/10.1021/jacs.7b11041.
[20] H. Kim, T. Yoon, Y. Kim, S. Hwang, J.H. Ryu, S.M. Oh, Increase of both solubility and working voltage by acetyl substitution on ferrocene for non-aqueous flow battery, Electrochem. Commun. 69 (2016) 72–75, https://doi.org/10.1016/j.elecom.2016.06.002.
[21] S. Hwang, H. seung Kim, J.H. Ryu, S.M. Oh, N-ferrocenylphthalimide; A single redox couple formed by attaching a ferrocene moiety to phthalimide for non-aqueous flow batteries, J. Power Sources 395 (2018) 60–65, https://doi.org/10.1016/j.jpowsour.2018.05.053.
[22] Y. Ding, Y. Zhao, Y. Li, J.B. Goodenough, G. Yu, A high-performance all-metallocene-based, non-aqueous redox flow battery, Energy Environ. Sci. 10 (2017) 491–497, https://doi.org/10.1039/C6EE02057G.
[23] M. Milton, Q. Cheng, Y. Yang, C. Nuckolls, R. Hernández Sánchez, T.J. Sisto, Molecular materials for nonaqueous flow batteries with a high coulombic efficiency and stable cycling, Nano Lett. 17 (2017) 7859–7863, https://doi.org/10.1021/acs.nanolett.7b04131.
[24] B.R. Schrage, Z. Zhao, C.J. Ziegler, A. Boika, Cation-anion redox switching in an all-ferrocene salt, ChemElectroChem 5 (2018) 3624–3627, https://doi.org/10.1002/celc.201801035.
[25] K. Chanawanno, C. Holstrom, L.A. Crandall, H. Dodge, V.N. Nemykin, R.S. Herrick, C.J. Ziegler, The synthesis and structures of 1,1′-bis(sulfonyl) ferrocene derivatives, Dalt. Trans. 45 (2016) 14320–14326, https://doi.org/10.1039/C6DT02669A.
[26] D.W. Slocum, W. Achermann, The preparation of several N-substituted and N,N-substituted ferrocenesulfonamides, Synth. React. Inorg. Met. Chem. 12 (1982) 397–405.
[27] G.M. Sheldrick, A short history of SHELX, Acta Crystallogr. Sect. A Found. Crystallogr. 64 (2008) 112–122, https://doi.org/10.1107/S0108767307043930.
[28] Y. Wen, Z. Cheng, W. Li, Z. Li, D. Liao, X. Hu, N. Pan, D. Wang, T.R. Hull, A novel oligomer containing DOPO and ferrocene groups: synthesis, characterization, and its application in fire retardant epoxy resin, Polym. Degrad. Stabil. 156 (2018) 111–124, https://doi.org/10.1016/j.polymdegradstab.2018.08.010.
[29] S. Chernyy, Z. Wang, J.J.K. Kirkensgaard, A. Bakke, K. Mortensen, S. Ndoni, K. Almdal, Synthesis and characterization of ferrocene containing block copolymers, J. Polym. Sci. Part A Polym. Chem. 55 (2017) 495–503, https://doi.org/10.1002/pola.28435.
[30] X. Peng, H. He, J. Xia, Z. Lou, G. Chang, X. Zhang, S. Wang, Visual detection and removal of mercury ions by a ferrocene derivative, Tetrahedron Lett. 55 (2014) 3541–3544, https://doi.org/10.1016/j.tetlet.2014.04.093. Wuhan, Hubei.
[31] N.S. Radulovic, M.Z. Mladenovic, Z. Stojanovic-Radic, G.A. Bogdanovic, D. Stevanovic, R.D. Vukicevic, Synthesis, characterization, and antimicrobial evaluation of a small library of ferrocene-containing acetoacetates and phenyl

analogs: the discovery of a potent anticandidal agent, Mol. Divers. 18 (2014) 497–510, https://doi.org/10.1007/s11030-014-9511-0.
[32] A. Federman Neto, J. Miller, V. Faria de Andrade, S.Y. Fujimoto, M.M.D.F. Afonso, F.C. Archanjo, V.A. Darin, M.L. Andrade e. Silva, A.D.L. Borges, G. Del Ponte, New synthesis of ferrocene monocarboxylic acid and systematic studies on the preparation of related key-intermediates, Zeitschrift Fuer Anorg. Und Allg. Chemie. 628 (2002) 209–216.
[33] P.L. Pauson, Ferrocene., in: E-EROS Encycl. Reagents Org. Synth., John Wiley & Sons, Ltd., 2001, pp. 1–5. http://onlinelibrary.wiley.com/doi/10.1002/047084289X.rf001/pdf.
[34] K. Chanawanno, T.S. Blesener, B.R. Schrage, V.N. Nemykin, R.S. Herrick, C.J. Ziegler, Amino acid ferrocene conjugates using sulfonamide linkages, J. Organomet. Chem. 870 (2018) 121–129, https://doi.org/10.1016/j.jorganchem.2018.06.018.
[35] K. Chanawanno, C. Holstrom, L.A. Crandall, H. Dodge, V.N. Nemykin, R.S. Herrick, C.J. Ziegler, The synthesis and structures of 1,1'-bis(sulfonyl) ferrocene derivatives, Dalt. Trans. 45 (2016) 14320–14326, https://doi.org/10.1039/C6DT02669A.
[36] P. Sahoo, V.G. Puranik, A.K. Patra, P.U. Sastry, P. Dastidar, Ferrocene based organometallic gelators: a supramolecular synthon approach, Soft Matter 7 (2011) 3634–3641, https://doi.org/10.1039/c0sm01148g.
[37] A.J. Blake, C. Caltagirone, V. Lippolis, M. Schroeder, C. Wilson, (Ferrocenylmethyl)trimethylammonium triiodide, Acta Crystallogr. Sect. E Struct 60 (2004) m20–m21, https://doi.org/10.1107/S1600536803026084. Reports Online.
[38] J. Xie, B.F. Abrahams, T.J. Zimmermann, A. Mukherjee, A.G. Wedd, Ferrocene mono- and di-sulfonates as building blocks in hydrogen-bonded networks, Aust. J. Chem. 60 (2007) 578–582, https://doi.org/10.1071/CH07072.
[39] G. Ferguson, J.F. Gallagher, C. Glidewell, C.M. Zakaria, Structures of (ferrocenylmethyl)trimethylammonium iodide and hexa-N-methylferrocene-1,1'-diylbis(methylammonium iodide), Acta Crystallogr. Sect. B Struct. Sci. B50 (1994) 146–150, https://doi.org/10.1107/S0108768193010985.
[40] C.M. Zakaria, G. Ferguson, A.J. Lough, C. Glidewell, Ferrocene-1,1'-dicarboxylic acid as a building block in supramolecular chemistry: supramolecular structures in one, two and three dimensions, Acta Crystallogr. Sect. B Struct. Sci. B58 (2002) 786–802, https://doi.org/10.1107/S010876810200976X.
[41] G. Cooke, F.M.A. Duclairoir, A. Kraft, G. Rosair, V.M. Rotello, Pronounced stabilization of the ferrocenium state of ferrocenecarboxylic acid by salt bridge formation with a benzamidine, Tetrahedron Lett. 45 (2004) 557–560, https://doi.org/10.1016/j.tetlet.2003.10.218.
[42] V.A. Russell, M.D. Ward, Two-dimensional hydrogen-bonded assemblies: the influence of sterics and competitive hydrogen bonding on the structures of guanidinium arenesulfonate networks, J. Mater. Chem. 7 (1997) 1123–1133, https://doi.org/10.1039/a700023e.
[43] Y. Wang, , supporting information, Acta Crystallogr. Sect. E. 68 (2012) 197, https://doi.org/10.1107/S1600536812002176.
[44] O. Reynes, J.-C. Moutet, J. Pecaut, G. Royal, E. Saint-Aman, (Ferrocenylmethyl) trimethylammonium cation: a very simple probe for the electro-chemical sensing of dihydrogen phosphate and ATP anions, New J. Chem. 26 (2002) 9–12, https://doi.org/10.1039/b107713a.
[45] B. Hu, C. DeBruler, Z. Rhodes, T.L. Liu, Long-cycling aqueous organic redox flow battery (AORFB) toward sustainable and safe energy storage, J. Am. Chem. Soc. 139 (2017) 1207–1214, https://doi.org/10.1021/jacs.6b10984.
[46] G.J. Tustin, V.G.H. Lafitte, C.E. Banks, T.G.J. Jones, R.B. Smith, J. Davis, N.S. Lawrence, Synthesis and characterisation of water soluble ferrocenes: molecular tuning of redox potentials, J. Organomet. Chem. 692 (2007) 5173–5182, https://doi.org/10.1016/j.jorganchem.2007.07.048.
[47] N.S. Lawrence, G.J. Tustin, M. Faulkner, T.G.J. Jones, Ferrocene sulfonates as electrocatalysts for sulfide detection, Electrochim. Acta 52 (2006) 499–503, https://doi.org/10.1016/j.electacta.2006.05.031.
[48] A.J. Bard, L.R. Faulkner, Electrochemical Methods : Fundamentals and Applications, second ed., John Wiley, New York ; Chichester [England], 2001.
[49] A. Singh, D.R. Chowdhury, A. Paul, A kinetic study of ferrocenium cation decomposition utilizing an integrated electrochemical methodology composed of cyclic voltammetry and amperometry, Anal. (Cambridge, United Kingdom) 139 (2014) 5747–5754, https://doi.org/10.1039/C4AN01325E.
[50] A.K. Vijh, B.E. Conway, Electrode kinetic aspects of the Kolbe reaction, Chem. Rev. 67 (1967) 623–664, https://doi.org/10.1021/cr60250a003. Washington, DC, United States.
[51] E. David R. Lide, CRC Handbook of Chemistry and Physics, Boca Raton, 2005. http://www.hbcpnetbase.com.